

1 **Genetic overlap between multivariate measures of human functional brain connectivity and**  
2 **psychiatric disorders**

3  
4 Daniel Roelfs<sup>1,\*</sup>, Dennis van der Meer<sup>1,2</sup>, Dag Alnæs<sup>1,3</sup>, Oleksandr Frei<sup>1,4</sup>, Alexey A. Shadrin<sup>1</sup>, Robert  
5 Loughnan<sup>5</sup>, Chun Chieh Fan<sup>6,7,8</sup>, Anders M. Dale<sup>9,8,10</sup>, Ole A. Andreassen<sup>1,11</sup>, Lars T. Westlye<sup>1,11,12</sup>, Tobias  
6 Kaufmann<sup>1,13\*</sup>

7  
8 <sup>1</sup> *NORMENT, Division of Mental Health and Addiction, Oslo University Hospital & Institute of Clinical*  
9 *Medicine, University of Oslo, Oslo, Norway*

10 <sup>2</sup> *School of Mental Health and Neuroscience, Faculty of Health, Medicine, and Life Sciences, Maastricht*  
11 *University, Maastricht, the Netherlands*

12 <sup>3</sup> *Björknes College, Oslo, Norway*

13 <sup>4</sup> *Center for Bioinformatics, Department of Informatics, University of Oslo, Oslo, Norway*

14 <sup>5</sup> *Department of Cognitive Science, University of California, San Diego, 9500 Gilman Drive, La Jolla, CA*  
15 *92093 USA*

16 <sup>6</sup> *Population Neuroscience and Genetics Lab, University of California, San Diego, CA, USA.*

17 <sup>7</sup> *Center for Human Development, University of California, San Diego, CA, USA*

18 <sup>8</sup> *Department of Radiology, School of Medicine, University of California, San Diego, CA, USA*

19 <sup>9</sup> *Department of Neurosciences, University of California San Diego, La Jolla, CA 92037, USA*

20 <sup>10</sup> *Center for Multimodal Imaging and Genetics, University of California at San Diego, La Jolla, CA,*  
21 *92037, USA*

22 <sup>11</sup> *K.G. Jebsen Center for Neurodevelopmental disorders, University of Oslo, Oslo, Norway*

23 <sup>12</sup> *Department of Psychology, University of Oslo, Oslo, Norway*

24 <sup>13</sup> *Department of Psychiatry and Psychotherapy, Tübingen Center for Mental Health, University of*  
25 *Tübingen, Germany*

26  
27 \* Correspondence: Daniel Roelfs & Tobias Kaufmann, PhD.

28 Email: [daniel.roelfs@medisin.uio.no](mailto:daniel.roelfs@medisin.uio.no), [tobias.kaufmann@medisin.uio.no](mailto:tobias.kaufmann@medisin.uio.no)

29 Postal address: OUS, PO Box 4956 Nydalen, 0424 Oslo, Norway

30 Telephone: +47 23 02 73 50, Fax: +47 23 02 73 33

31  
32 Counts: Main: 2732 words | Abstract: 135 words | Figures: 4 | References: 75

33

## Roelfs et al. | Genetics of the brain functional connectome

### 34 **Abstract**

35 Psychiatric disorders are complex, heritable, and highly polygenic. Supported by findings of abnormalities  
36 in functional magnetic resonance imaging (fMRI) based measures of brain connectivity, current  
37 theoretical and empirical accounts have conceptualized them as disorders of brain connectivity and  
38 dysfunctional integration of brain signaling, however, the extent to which these findings reflect common  
39 genetic factors remains unclear. Here, we performed a multivariate genome-wide association analysis of  
40 fMRI-based functional brain connectivity in a sample of 30,701 individuals from the UK Biobank and  
41 investigated the shared genetic determinants with seven major psychiatric disorders. The analysis revealed  
42 significant genetic overlap between functional brain connectivity and schizophrenia, bipolar disorder,  
43 attention-deficit hyperactivity disorder, autism spectrum disorder, anxiety, and major depression, adding  
44 further genetic support for the dysconnectivity hypothesis of psychiatric disorders and identifying  
45 potential genetic and functional targets for future studies.

## 46 **Introduction**

47 Psychiatric disorders are heritable and highly polygenic<sup>1-4</sup>, and carry a high burden of disease, measured  
48 in years lived with disability<sup>5</sup>. Akin to the polygenic architecture of the disorders, where a number of  
49 variants each contribute with small effects, findings from imaging genetics studies have documented a  
50 distributed pattern of small effects across the genome for brain phenotypes derived from magnetic  
51 resonance imaging (MRI)<sup>6</sup>. Likewise, brain imaging studies of psychiatric disorders have revealed  
52 distributed anatomical and functional alterations across the brain, with a large body of literature indicating  
53 alterations in functional brain connectivity in individuals with a range of psychiatric disorders, including  
54 schizophrenia (SCZ; e.g. Pettersson-Yeo et al., 2011<sup>7</sup>), bipolar disorder (BIP; e.g. Syan et al., 2018<sup>8</sup>),  
55 autism spectrum disorders (ASD; e.g. Hong et al., 2019<sup>9</sup>), attention-deficit hyperactivity disorder (ADHD;  
56 e.g. Gao et al., 2019<sup>10</sup>), major depression (MDD; e.g. Brakowski et al., 2017<sup>11</sup>), post-traumatic stress  
57 disorder (PTSD; e.g. Akiki et al., 2017<sup>12</sup>) and anxiety disorders (ANX; e.g. Xu et al., 2019<sup>13</sup>).

58 Altered brain connectivity in psychiatric disorders might reflect changes in synaptic functioning.  
59 Evidence from induced pluripotent stem cell research shows that mutations relevant to psychiatric  
60 disorders cause synapse deficits<sup>14</sup>, genome-wide association studies (GWAS) of psychiatric disorders  
61 identified various genes involved in synaptic functioning<sup>4,15-17</sup>, and gene expression studies identified  
62 differential expression patterns in synapse related genes in these disorders<sup>18</sup>.

63 While both neuroimaging and genetic studies each have pointed to synaptic alterations in psychiatric  
64 disorders, only a few have specifically tested this hypothesis in an integrated imaging-genetics framework.  
65 A few studies have explored the genetic architecture of functional brain connectivity<sup>19-23</sup>, and studies  
66 assessing polygenic risk scores have indicated links between psychiatric disorders and abnormal brain  
67 connectivity<sup>24,25</sup>. Previous studies also illustrated genetic correlation between various brain imaging  
68 phenotypes and psychiatric disorders that confirm a large degree of shared effect sizes across single  
69 nucleotide polymorphisms (SNPs)<sup>26-28</sup>. However, we still lack a concise map of the overlap in genetic  
70 architecture between psychiatric disorders and the brain functional connectome.

71 Recent evidence from anatomical imaging suggests a distributed nature of genetic effects on the brain,  
72 calling for tools that take a multivariate approach to imaging genetics, beyond univariate genome-wide  
73 association studies of single brain phenotypes<sup>29</sup>. We hypothesized that such distributed nature of genetic  
74 effects is also observable in the genetic architecture of functional imaging given the functional interplay of  
75 brain regions (nodes) in the connectome. A multivariate approach would perform better at capturing these  
76 distributed effects than conventional univariate GWAS<sup>29</sup>. Using data from the UK Biobank, we therefore  
77 deployed such approach to study the genetic architecture of functional brain connectivity – here defined as  
78 the correlation between time series data of large-scale brain network nodes<sup>30,31</sup>. Based on previous  
79 research pointing at dysconnectivity in psychiatric disorders, we expected that there is overlapping genetic  
80 architecture between the functional connectome and the disorders that can be captured using our

81 multivariate approach. We therefore assessed genetic overlap between the connectome and seven major  
82 psychiatric disorders (ADHD, ANX, ASD, BIP, MDD, PTSD and SCZ; Suppl. Table 1).

83

## 84 **Results**

85 We performed two multivariate GWAS using the Multivariate Omnibus Statistical Test  
86 (MOSTest)<sup>29</sup>, one based on connectivity of 210 connections between 21 large-scale brain network nodes,  
87 and one based on signal variance across time in the respective 21 nodes. The two measures (connectivity  
88 and node variance) are mathematically related, yet as they operate at different levels of investigation (edge  
89 level (the connections) vs. node level) they may deliver complementary insights. The main analysis  
90 included data from 30,701 white British individuals aged 45-82 years (52.8% females) and replication  
91 analysis included an independent sample of 9154 individuals aged 45-83 (52.9% female). The Miami plots  
92 in Figure 1A illustrate the multivariate genetic associations calculated using MOSTest, and for  
93 comparison the associations identified using the traditional min-p approach, which takes the smallest p-  
94 value across univariate GWASs. Supplementary Figure 1 depicts corresponding QQ-Plots. MOSTest  
95 identified 15 genetic loci significantly ( $P < 5e-8$ ) associated with functional brain connectivity (FC) and 5  
96 loci significantly associated with node variance (Suppl. Table 2), whereas the min-p approach only  
97 identified 2 loci for FC and 3 loci for node variance. Four of the five loci identified for node variance were  
98 also present for FC, in line with the phenotypic relationship between the two. In the independent  
99 replication sample, loci replicated well at nominal p-value, with 14 of 15 connectivity loci and all node  
100 variance loci replicating at  $P < .05$  (Suppl. Fig. 2). Furthermore, to test whether the method by which we  
101 derived the functional brain measures affected the results, we supplemented our data-driven ICA approach  
102 with a separate ROI-based pipeline, where we defined brain networks using a region-of-interest approach  
103 (see *Online Methods*). Results of these analyses indicate converging results despite an independent  
104 processing pipeline and network definition approach (Suppl. Fig. 3, Suppl. Table 3).

105 The bottom row in Figure 1A shows individual univariate p-values for the MOSTest-discovered  
106 loci, illustrating that the univariate approach is only good at capturing strong effects (e.g. locus 3 for FC),  
107 yet fails to discover loci with enriched signal across brain phenotypes. This also indicates that signal  
108 captured by the min-p approach reflects mostly the effect of individual phenotypes, rather than the  
109 combined signal as captured by MOSTest. Figure 1B further illustrates the distributed nature of effects  
110 across the brain, where a given locus shows differential patterns of regional SNP effects. Finally, genetic  
111 correlation analysis of univariate node variance GWAS (Suppl. Fig. 4) illustrated strong genetic  
112 correlations between different brain network nodes, largely in line with the phenotypic correlations  
113 observed when correlating the fMRI time series, adding further support to a distributed nature of effects in  
114 fMRI-based connectomics.

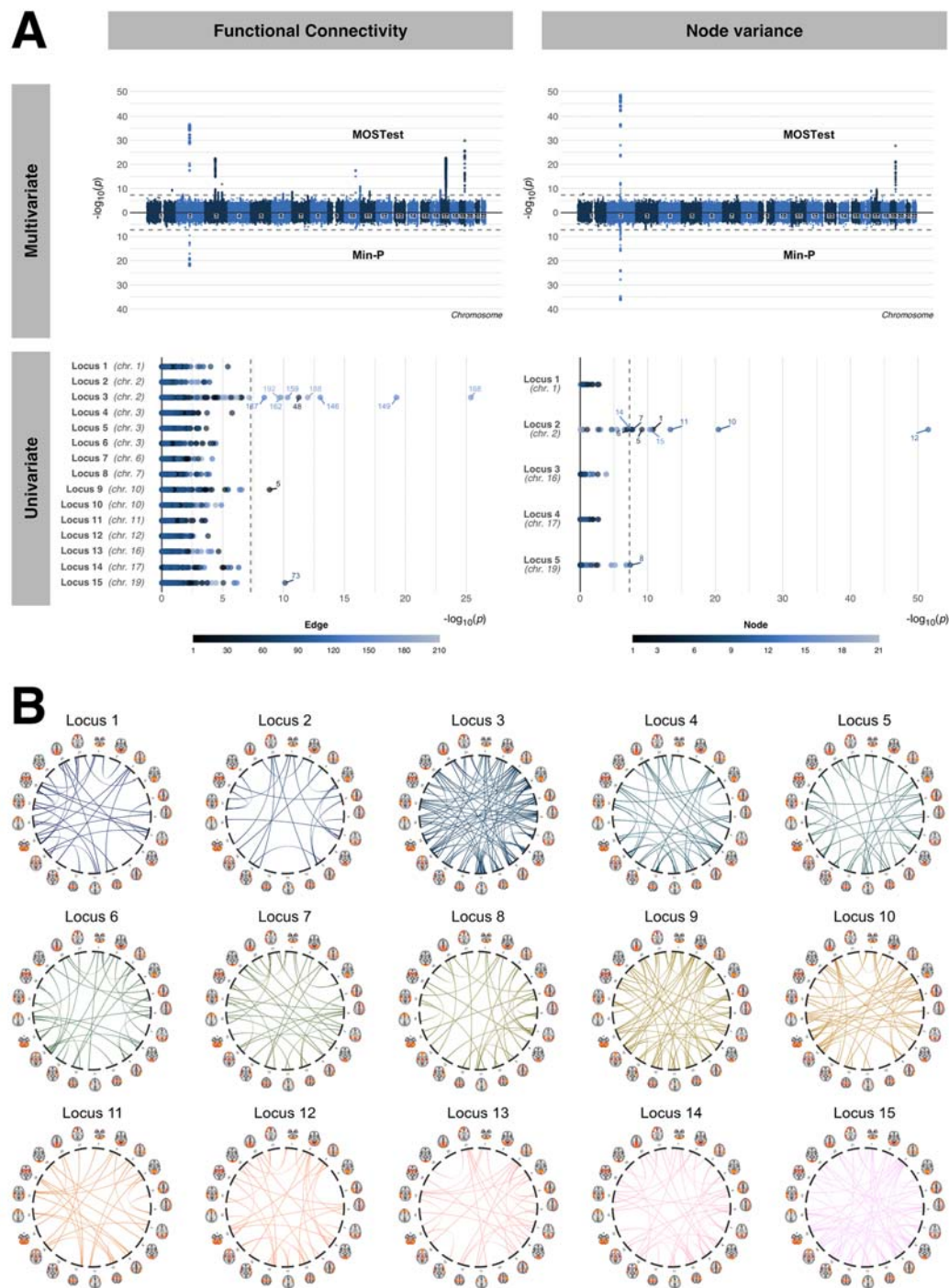


**Figure 1. Multivariate and univariate architecture of the brain functional connectome highlight a distributed nature of effects across the brain.** (A) The left column of the figure illustrates the results for functional brain connectivity, the right column for node variance. The first row shows Miami plots with the multivariate GWAS results from the MOSTest approach in the top, and the results from the traditional min-p approach at the bottom. The second row shows for each locus identified by MOSTest, the univariate p-values of

the lead SNP in each locus. A majority of loci identified by the multivariate approach were not detected via the univariate approach. (B) For each of the genome-wide significant loci underlying functional brain connectivity identified using the multivariate MOSTest approach, this panel shows nominally significant ( $P < 0.05$ ) connections from corresponding univariate statistics. These figures show differential patterns of regional SNP effects and highlight the distributed nature of the genetic effects on connectivity.

115  
116 To complement the multivariate stream, we further analyzed the univariate GWAS for each  
117 connection in the full brain network and for each node variance separately. Figure 2 depicts the SNP-  
118 based heritability for each connection (panel A) and for each node (panel B). SNP-based heritability  
119 ranged from 0.14% to 10.58% for brain connectivity (for 7 connections it could not be computed) and 137  
120 out of 210 connections had a heritability above 1.96 times its standard error, indicating genetic signal<sup>32</sup>.  
121 The connection with the highest heritability was the connection between nodes reflecting activity in the  
122 prefrontal cortex (network 16) and the frontal network (network 14). For node variance, SNP-based  
123 heritability ranged from 3.92% to 13.64% with all nodes above 1.96 times their standard error, and highest  
124 heritability observed for node 9 (temporo-parietal network). Univariate analysis revealed no significant  
125 loci for any of the nodes or edges when controlling for the total number of edges or nodes through  
126 Bonferroni correction. The number of significant loci for the multivariate stream compared to the  
127 univariate stream adds further support that the genetic signal is distributed across the brain functional  
128 connectome, allowing us to capitalize on the shared signal for loci discovery.  
129

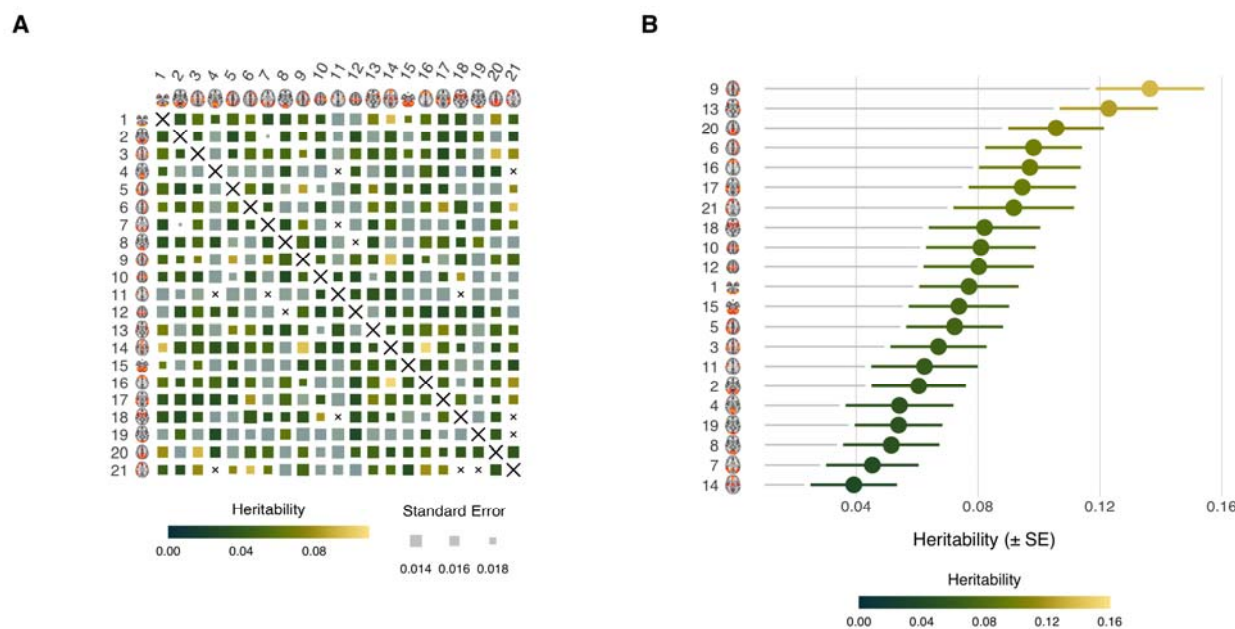


**Figure 2. Heritability across edges and nodes.** (A) SNP-based heritability ( $h^2$ ) for the 210 edges. Upper half and lower halves of the figure are identical. Dark green indicates lowest heritability, bright yellow indicates highest

## Roelfs et al. | Genetics of the brain functional connectome

heritability. Edges that did not survive heritability threshold are greyed out. Edges for which heritability could not be calculated are marked with a cross. (B)  $h^2$  for the 21 nodes. Color scheme follows panel A and standard errors are depicted as bars.

130  
131           Next, we tested for overlap between the two MOSTest-derived genetic profiles (functional  
132 connectivity and node variance) with seven major psychiatric disorders (ADHD, ASD, ANX, BIP, MD,  
133 PTSD, SCZ) using conjunctive FDR analysis<sup>33</sup>. As shown in Figure 3, we found shared loci for six of  
134 the seven disorders, namely for ADHD, ASD, ANX, MD, BIP and SCZ. By far the largest number of  
135 shared loci was implicated for SCZ (43 for FC, 22 for node variance). We found 6 loci for FC and 1 locus  
136 for node variance in ADHD, 9 loci for FC and 2 loci for node variance in BIP, and 4 loci for FC and 3 loci  
137 for node variance in ASD. Additionally, we found 1 shared locus between FC and MDD, and 1 shared  
138 locus between node variance and ANX. We did not find any shared loci between either FC or node  
139 variance and PTSD. Supplementary Fig. 5 depicts quantile-quantile plots for all genetic overlap analyses.  
140 Additional sensitivity analyses using a more stringent FDR threshold confirmed largest overlap for SCZ  
141 with FC among the traits (Suppl. Table 4). Analysis with a negative control trait (vitamin D levels:  $N =$   
142  $79,366$ )<sup>34</sup> yielded no significant overlap for node variance and two loci for connectivity (Suppl. Fig. 6).

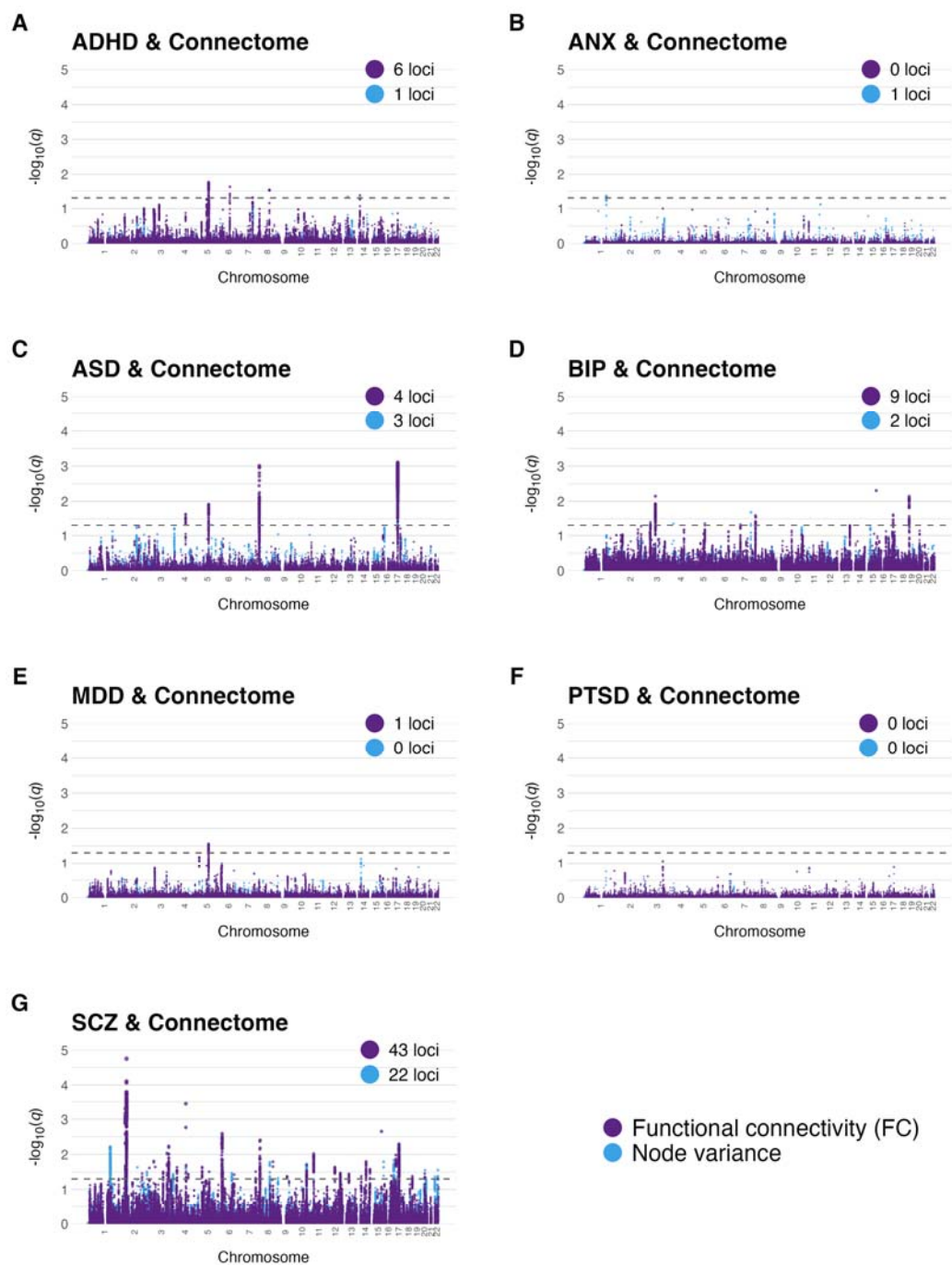


**Figure 3. Manhattan plots illustrating genetic overlap between disorders and the multivariate functional brain phenotypes.** Association strength per locus is depicted as q-value from the conjunctural FDR analysis<sup>35</sup>. Values for FC and node variance are shown in the same figure with separate colors.

143  
144 Using Functional Mapping and Annotation of GWAS (FUMA)<sup>36</sup>, we mapped the loci shared  
145 between the connectome and the psychiatric disorders to 180 genes, listed in Suppl. Table 5. We tested for



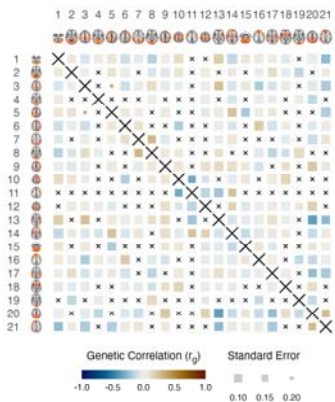
## Roelfs et al. | Genetics of the brain functional connectome

146 enrichment for biological processes (GO) and identified 125 significant associations, many of which are  
147 relevant to neural system development and functioning (Suppl. Fig. 7). Using *SynGO*<sup>37</sup>, we linked 23 of  
148 the 180 genes to synapse functioning (Suppl. Table 6). For example, one of the loci shared between SCZ  
149 and FC was mapped to BDNF, which is a major regulator of synaptic transmission and synaptic  
150 plasticity<sup>38</sup>. Another example is NRXN1, found also for SCZ and FC, which is known for its role in the  
151 formation of synaptic contacts<sup>39</sup>. Utilizing the pathway browser on the identified gene sets<sup>40</sup>, we also  
152 found that the mapped genes were involved in cell signaling and signal transduction, more specifically  
153 protein-protein interactions at the synapses, WNT and NTRK signaling, but also a number of other  
154 biological processes such as chromosome maintenance and mitosis (Suppl. Fig. 8 and Suppl. Table 7).

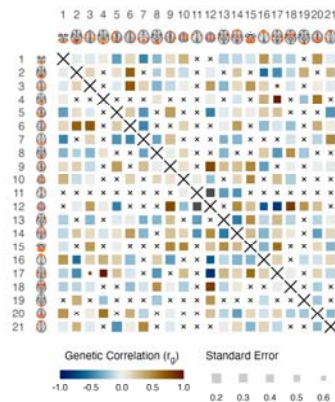
155 In addition to the conjunctive FDR analyses, we also calculated genetic correlation between  
156 each connection or node surviving our pre-defined threshold of 1.96 times its SE, and the seven  
157 psychiatric disorders. Figure 4A illustrates that genetic correlation was generally low for the connectome  
158 and only one connection survived after correcting for all seven disorders and all connections, specifically  
159 a connection between the right ventral (network 21) and the prefrontal network (network 16) was  
160 significantly associated with BIP ( $r_g = -0.25$ ,  $p_{\text{BONF}} = 0.0006$ ). When only correcting for the number of  
161 connections but not for the number of disorders, we found an additional significant association, which was  
162 the link between the auditory (network 17) and the subcortical (network 18) node which correlated with  
163 SCZ ( $r_g = 0.25$ ,  $p_{\text{BONF}} = 0.0137$ ). For node variance, we found two significant associations when correcting  
164 for all disorders and nodes. Specifically, variance in the temporo-parietal network (network 9) was  
165 significantly correlated with both, SCZ ( $r_g = 0.22$ ,  $p_{\text{BONF}} = 3.9\text{e-}6$ ) and BIP ( $r_g = 0.17$ ,  $p_{\text{BONF}} = 0.03$ ).

Roelfs et al. | Genetics of the brain functional connectome

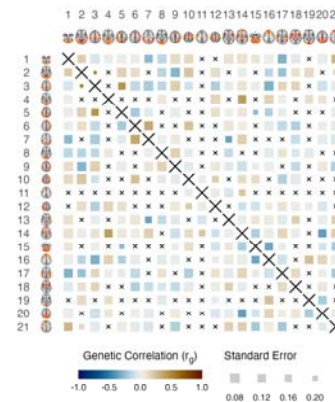
A.1 ADHD



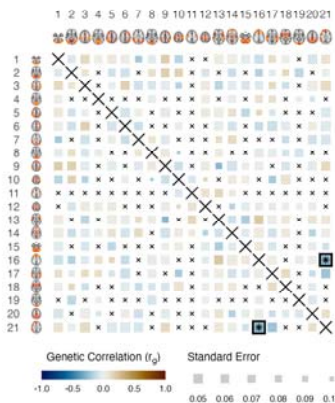
A.2 ANX



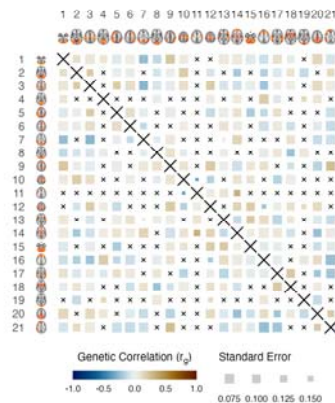
A.3 ASD



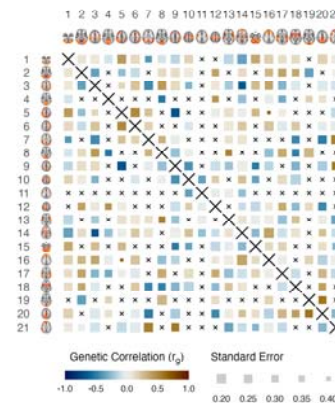
A.4 BIP



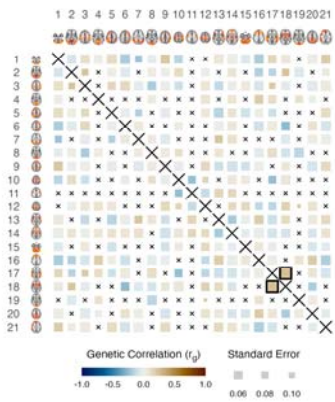
A.5 MDD



A.6 PTSD



A.7 SCZ



Roelfs et al. | Genetics of the brain functional connectome

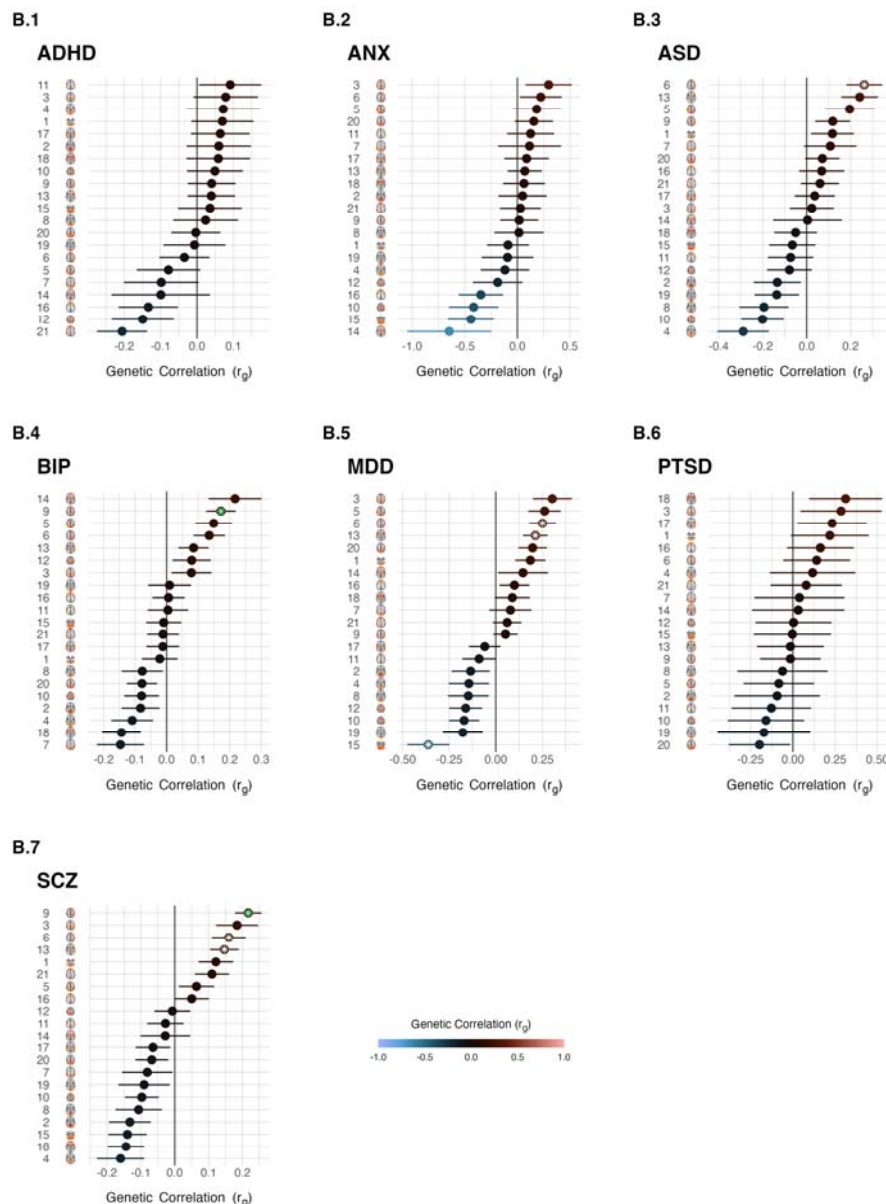


**Figure 4. Genetic correlation between the connectome and psychiatric disorders.** (A) The tiles show the genetic correlations between each edge of the whole brain network and a given psychiatric disorder. Size of the tile represents the standard error. Edges with a heritability below 1.96 its standard error were not considered in the analysis and marked with a black cross. Among all disorders, only one edge marked with a black border was significant for SCZ after correcting for the number of edges (210), whereas none was significant when correcting for the number of edges and the number of disorders. Upper and lower half of each matrix are identical. (B) Genetic correlation analysis at the node level. Significant genetic correlations within a psychiatric disorder are indicated with a white asterisk when correcting for the number of nodes, whereas a green asterisk indicates significance when correcting for both, the number of nodes and the number of disorders. The latter stringent correction was surpassed for variance of the temporo-parietal node and SCZ.

167 **Discussion**

168 Taken together, our study provided insight into the shared genetic architecture between measures of the  
169 brain functional connectome and common psychiatric disorders. Deploying multivariate genetic analyses  
170 of fMRI data from more than 30,000 individuals allowed us to capitalize on the distributed nature of  
171 genetic variation across the interconnected whole brain network to discover novel connectome-associated  
172 variants beyond what can be discovered using standard univariate approaches. Our analyses pinpointed a  
173 number of gene variants overlapping between the connectome and psychiatric disorders, where several of  
174 the corresponding mapped genes are known for their involvement with synapse formation and  
175 functioning.

176 We used two measures of the brain functional connectome – the 210 correlations of brain signal from  
177 21 nodes as measures of functional brain connectivity as well as signal variation across time of these 21  
178 network nodes. Given the interconnectedness of the connectome, we hypothesized that many connections  
179 or nodes would have overlapping genetic signatures. Indeed, our results illustrate that the genetic  
180 architecture of brain function is distributed across the brain. Our deployed multivariate approach  
181 successfully leveraged this pleiotropy for discovery, revealing a variety of genetic effects that would not  
182 have been discovered with the standard univariate GWAS approach, including the commonly used min-p  
183 approach, which identifies the minimum p-value across univariate GWASs. We observed that the  
184 significant lead SNPs from MOSTest were often not significantly associated with the univariate measure.  
185 This demonstrates that using multivariate genetic analysis can be valuable to complement the univariate  
186 approach in settings like brain imaging where the signal is largely distributed.

187 From our multivariate signatures of the connectome, we were able to identify a number of shared loci  
188 with psychiatric disorders through conjunctive FDR analysis. The strongest overlap was implied for  
189 schizophrenia yet all other psychiatric disorders apart from PTSD showed some degree of overlap as well,  
190 in particular with connectivity. Identification of overlap to some degree depends on sample sizes, which  
191 may for example explain the lack of findings for PTSD. However, it is important to note that sample size  
192 alone cannot explain the observed differences in overlapping loci. The bipolar disorder and schizophrenia  
193 GWASs have similar sample sizes yet we discovered many more loci for the latter. Likewise, our negative  
194 control analysis of a well powered trait yielded only two overlapping loci for connectivity and no  
195 significant locus for node variance. How the comparison between all disorders will look at similar power  
196 remains to be investigated.

197 Several synapse-related genes were among the overlapping genes, including some involved in the  
198 neurodevelopmental formation of synapses. This is particularly intriguing given that many psychiatric  
199 disorders are conceptualized as neurodevelopmental disorders even if they are typically diagnosed in  
200 adulthood. Further, many disorders are conceptualized as disorders of brain dysconnectivity, as initially

201 proposed for schizophrenia<sup>41</sup>. This is now established across various disorders<sup>42</sup> and our results provide  
202 further evidence from the genetics end.

203 We provided univariate analyses in addition to the multivariate stream and showed a map of genetic  
204 correlations between connectivity, node variance and psychiatric disorders. Univariate correlations were  
205 overall weak and only a few edges or nodes were significant after correcting for multiple testing.  
206 Therefore, caution is warranted when interpreting potential disorder-specific patterns observed in the  
207 univariate analysis. Lack of genetic correlating does not necessarily indicate lack of polygenic overlap, as  
208 shown previously by multiple methods, including cross-trait MiXeR analysis<sup>43</sup> and LAVA<sup>44</sup>. It is well  
209 possible that a variety of SNPs with opposing effect directions cancel each other out, which would result  
210 in low genetic correlation despite genetic overlap. The finding that genetic correlations from univariate  
211 analyses are relatively weak despite significant genetic overlap between our multivariate GWAS and  
212 several psychiatric disorders provides further evidence that multivariate analysis is an important method to  
213 dissect complex interactions in psychiatric genetics.

214 We here provided results from analyses at the edge level (functional connectivity) and node level  
215 (node variance). The latter showed larger heritability and larger effect sizes than functional connectivity.  
216 This may be partly explained by the granularity of the connectivity measure, its partial correlation account  
217 for all other edges in the network, or a better representation of the nodes across individuals compared to  
218 the potentially highly individualized network configurations<sup>45,46</sup>. At the phenotypic level, node variance  
219 has been associated with psychiatric disorders, with effect sizes comparable to connectivity<sup>47-49</sup>. Given  
220 that our genetic analyses often imply similar genes for node-level and connectivity-level, the underlying  
221 sources may align despite differences in current association effect sizes.

222 Some aspects are relevant for interpreting the current findings. First, MOSTest is to some degree  
223 dependent on granularity as also previously shown<sup>50</sup> which may explain why MOSTest identified more  
224 loci for functional connectivity than for node variance. More research using different approaches to  
225 network definition may yield further discoveries, however, our comparison of the genetic architecture of  
226 ICA-based and ROI-based networks also indicated large overlap, supporting robustness of the current  
227 findings. Second, lack of effect directionality is a limitation of the multivariate analysis, which is why we  
228 provided univariate analyses alongside. Furthermore, several post-GWAS analyses such as for example  
229 the conjunctive FDR framework do not require effect direction and can thus be performed with the  
230 resulting multivariate statistics. We believe the strengths of the multivariate approach outweigh the  
231 limitations, and a tandem approach with both multivariate and univariate methods optimizes utility of this  
232 method. Finally, with conjunctive FDR analysis it can happen that some discoveries are novel, meaning  
233 they are missed by standard GWAS due to lack of power or excessive burden of multiple testing.  
234 However, it is expected that conjunctive FDR loci will be discovered by these standard GWAS  
235 methodology once sample sizes increase further. For example, two loci recently discovered in a GWAS on

236 ADHD<sup>51</sup> were already discovered earlier using a conjunctive FDR analysis with educational  
237 attainment<sup>52</sup>.

238 In conclusion, we here revealed a distributed nature of genetic effects on brain function and  
239 integration, and identified a number of genetic loci associated with key properties of the brain functional  
240 connectome. Further, we revealed a large degree of genetic overlap between multivariate measures of the  
241 brain functional connectome and a number of psychiatric disorders with genes pointing at synaptic  
242 plasticity. This may help further disentangle the complex biological underpinnings of psychiatric disorders  
243 and provide a bridge between functional connectivity alterations and genetic variations in patients. There  
244 is a need for follow-up experimental studies building on the discovered loci to disentangle the biological  
245 mechanisms.

246

## 247 **References**

248

- 249 1. Anttila, V. *et al.* Analysis of shared heritability in common disorders of the brain. *Science* **360**,  
250 eaap8757 (2018).
- 251 2. Fullerton, J. M. & Nurnberger, J. I. Polygenic risk scores in psychiatry: Will they be useful for  
252 clinicians? *F1000Research* **8**, (2019).
- 253 3. Smoller, J. W. *et al.* Psychiatric genetics and the structure of psychopathology. *Mol. Psychiatry* **24**,  
254 409–420 (2019).
- 255 4. Sullivan, P. F. & Geschwind, D. H. Defining the Genetic, Genomic, Cellular, and Diagnostic  
256 Architectures of Psychiatric Disorders. *Cell* **177**, 162–183 (2019).
- 257 5. Vos, T. *et al.* Global burden of 369 diseases and injuries in 204 countries and territories, 1990–2019: a  
258 systematic analysis for the Global Burden of Disease Study 2019. *The Lancet* **396**, 1204–1222 (2020).
- 259 6. Paulus, M. P. & Thompson, W. K. The Challenges and Opportunities of Small Effects: The New  
260 Normal in Academic Psychiatry. *JAMA Psychiatry* **76**, 353–354 (2019).
- 261 7. Pettersson-Yeo, W., Allen, P., Benetti, S., McGuire, P. & Mechelli, A. Dysconnectivity in  
262 schizophrenia: where are we now? *Neurosci. Biobehav. Rev.* **35**, 1110–1124 (2011).
- 263 8. Syan, S. K. *et al.* Resting-state functional connectivity in individuals with bipolar disorder during  
264 clinical remission: a systematic review. *J. Psychiatry Neurosci. JPN* **43**, 298–316 (2018).

Roelfs et al. | Genetics of the brain functional connectome

- 265 9. Hong, S.-J. *et al.* Atypical functional connectome hierarchy in autism. *Nat. Commun.* **10**, 1022 (2019).
- 266 10. Gao, Y. *et al.* Impairments of large-scale functional networks in attention-deficit/hyperactivity  
267 disorder: a meta-analysis of resting-state functional connectivity. *Psychol. Med.* **49**, 2475–2485  
268 (2019).
- 269 11. Brakowski, J. *et al.* Resting state brain network function in major depression - Depression  
270 symptomatology, antidepressant treatment effects, future research. *J. Psychiatr. Res.* **92**, 147–159  
271 (2017).
- 272 12. Akiki, T. J., Averill, C. L. & Abdallah, C. G. A Network-Based Neurobiological Model of PTSD:  
273 Evidence From Structural and Functional Neuroimaging Studies. *Curr. Psychiatry Rep.* **19**, 81 (2017).
- 274 13. Xu, J. *et al.* Anxious brain networks: A coordinate-based activation likelihood estimation meta-  
275 analysis of resting-state functional connectivity studies in anxiety. *Neurosci. Biobehav. Rev.* **96**, 21–  
276 30 (2019).
- 277 14. Wen, Z. *et al.* Synaptic dysregulation in a human iPSC cell model of mental disorders. *Nature* **515**,  
278 414–418 (2014).
- 279 15. Devor, A. *et al.* Genetic evidence for role of integration of fast and slow neurotransmission in  
280 schizophrenia. *Mol. Psychiatry* **22**, 792–801 (2017).
- 281 16. Howard, D. M. *et al.* Genome-wide association study of depression phenotypes in UK Biobank  
282 identifies variants in excitatory synaptic pathways. *Nat. Commun.* **9**, 1470 (2018).
- 283 17. Ripke, S., Walters, J. T. & O'Donovan, M. C. Mapping genomic loci prioritises genes and implicates  
284 synaptic biology in schizophrenia. *medRxiv* 2020.09.12.20192922 (2020)  
285 doi:10.1101/2020.09.12.20192922.
- 286 18. Lopez de Lara, C. *et al.* Implication of synapse-related genes in bipolar disorder by linkage and gene  
287 expression analyses. *Int. J. Neuropsychopharmacol.* **13**, 1397–1410 (2010).
- 288 19. Aurina Arnatkeviciute, Ben Fulcher, Mark Bellgrove, & Alex Fornito. Where the Genome Meets the  
289 Connectome: Understanding How Genes Shape Human Brain Connectivity. *PsyArXiv* (2021)  
290 doi:<https://doi.org/10.31234/osf.io/hqgz7>.

Roelfs et al. | Genetics of the brain functional connectome

- 291 20. Barabási, D. L. & Barabási, A.-L. A Genetic Model of the Connectome. *Neuron* **105**, 435-445.e5  
292 (2020).
- 293 21. Fornito, A. *et al.* Genetic influences on cost-efficient organization of human cortical functional  
294 networks. *J. Neurosci. Off. J. Soc. Neurosci.* **31**, 3261–3270 (2011).
- 295 22. Smith, S. M. *et al.* An expanded set of genome-wide association studies of brain imaging phenotypes  
296 in UK Biobank. *Nat. Neurosci.* (2021) doi:10.1038/s41593-021-00826-4.
- 297 23. Yang, Z. *et al.* Genetic and Environmental Contributions to Functional Connectivity Architecture of  
298 the Human Brain. *Cereb. Cortex N. Y. N 1991* **26**, 2341–2352 (2016).
- 299 24. Cao, H., Zhou, H. & Cannon, T. D. Functional connectome-wide associations of schizophrenia  
300 polygenic risk. *Mol. Psychiatry* (2020) doi:10.1038/s41380-020-0699-3.
- 301 25. Miller, D. R. *et al.* Posttraumatic stress disorder symptom severity is associated with reduced default  
302 mode network connectivity in individuals with elevated genetic risk for psychopathology. *Depress.*  
303 *Anxiety* **34**, 632–640 (2017).
- 304 26. Hibar, D. P. *et al.* Cortical abnormalities in bipolar disorder: an MRI analysis of 6503 individuals  
305 from the ENIGMA Bipolar Disorder Working Group. *Mol. Psychiatry* **23**, 932–942 (2018).
- 306 27. Walton, E. *et al.* Exploration of Shared Genetic Architecture Between Subcortical Brain Volumes and  
307 Anorexia Nervosa. *Mol. Neurobiol.* **56**, 5146–5156 (2019).
- 308 28. Zhao, B. *et al.* Large-scale GWAS reveals genetic architecture of brain white matter microstructure  
309 and genetic overlap with cognitive and mental health traits (n = 17,706). *Mol. Psychiatry* (2019)  
310 doi:10.1038/s41380-019-0569-z.
- 311 29. van der Meer, D. *et al.* Understanding the genetic determinants of the brain with MOSTest. *Nat.*  
312 *Commun.* **11**, 3512 (2020).
- 313 30. Smith, S. M. *et al.* Network modelling methods for FMRI. *NeuroImage* **54**, 875–891 (2011).
- 314 31. Smitha, K. A. *et al.* Resting state fMRI: A review on methods in resting state connectivity analysis  
315 and resting state networks. *Neuroradiol. J.* **30**, 305–317 (2017).



Roelfs et al. | Genetics of the brain functional connectome

- 316 32. Shi, H., Mancuso, N., Spendlove, S. & Pasaniuc, B. Local Genetic Correlation Gives Insights into the  
317 Shared Genetic Architecture of Complex Traits. *Am. J. Hum. Genet.* **101**, 737–751 (2017).
- 318 33. Smeland, O. B. *et al.* Discovery of shared genomic loci using the conditional false discovery rate  
319 approach. *Hum. Genet.* **139**, 85–94 (2020).
- 320 34. Jiang, X. *et al.* Genome-wide association study in 79,366 European-ancestry individuals informs the  
321 genetic architecture of 25-hydroxyvitamin D levels. *Nat. Commun.* **9**, 260 (2018).
- 322 35. Andreassen, O. A. *et al.* Improved detection of common variants associated with schizophrenia and  
323 bipolar disorder using pleiotropy-informed conditional false discovery rate. *PLoS Genet* **9**, e1003455  
324 (2013).
- 325 36. Watanabe, K., Taskesen, E., van Bochoven, A. & Posthuma, D. Functional mapping and annotation of  
326 genetic associations with FUMA. *Nat. Commun.* **8**, 1826 (2017).
- 327 37. Koopmans, F. *et al.* SynGO: An Evidence-Based, Expert-Curated Knowledge Base for the Synapse.  
328 *Neuron* **103**, 217-234.e4 (2019).
- 329 38. Dean, C. *et al.* Synaptotagmin-IV modulates synaptic function and long-term potentiation by  
330 regulating BDNF release. *Nat. Neurosci.* **12**, 767–776 (2009).
- 331 39. Dean, C. *et al.* Neurexin mediates the assembly of presynaptic terminals. *Nat. Neurosci.* **6**, 708–716  
332 (2003).
- 333 40. Jassal, B. *et al.* The reactome pathway knowledgebase. *Nucleic Acids Res.* **48**, D498–D503 (2020).
- 334 41. Friston, K., Brown, H. R., Siemerikus, J. & Stephan, K. E. The dysconnection hypothesis (2016).  
335 *Schizophr. Res.* **176**, 83–94 (2016).
- 336 42. van den Heuvel, M. P. & Sporns, O. A cross-disorder connectome landscape of brain dysconnectivity.  
337 *Nat. Rev. Neurosci.* **20**, 435–446 (2019).
- 338 43. Frei, O. *et al.* Bivariate causal mixture model quantifies polygenic overlap between complex traits  
339 beyond genetic correlation. *Nat. Commun.* **10**, 2417–2417 (2019).
- 340 44. Werme, J., van der Sluis, S., Posthuma, D. & de Leeuw, C. A. LAVA: An integrated framework for  
341 local genetic correlation analysis. *bioRxiv* 2020.12.31.424652 (2021) doi:10.1101/2020.12.31.424652.

Roelfs et al. | Genetics of the brain functional connectome

- 342 45. Finn, E. S. *et al.* Functional connectome fingerprinting: identifying individuals using patterns of brain  
343 connectivity. *Nat. Neurosci.* **18**, 1664–1671 (2015).
- 344 46. Kaufmann, T. *et al.* Delayed stabilization and individualization in connectome development are  
345 related to psychiatric disorders. *Nat. Neurosci.* **20**, 513–515 (2017).
- 346 47. Kaufmann, T. *et al.* Disintegration of Sensorimotor Brain Networks in Schizophrenia. *Schizophr.*  
347 *Bull.* **41**, 1326–1335 (2015).
- 348 48. Lynall, M.-E. *et al.* Functional connectivity and brain networks in schizophrenia. *J. Neurosci. Off. J.*  
349 *Soc. Neurosci.* **30**, 9477–9487 (2010).
- 350 49. Rolls, E. T., Cheng, W. & Feng, J. Brain dynamics: the temporal variability of connectivity, and  
351 differences in schizophrenia and ADHD. *Transl. Psychiatry* **11**, 70 (2021).
- 352 50. Shadrin, A. A. *et al.* Multivariate genome-wide association study identifies 780 unique genetic loci  
353 associated with cortical morphology. *bioRxiv* 2020.10.22.350298 (2021)  
354 doi:10.1101/2020.10.22.350298.
- 355 51. Demontis, D. *et al.* Discovery of the first genome-wide significant risk loci for attention  
356 deficit/hyperactivity disorder. *Nat. Genet.* **51**, 63–75 (2019).
- 357 52. Shadrin, A. A. *et al.* Novel Loci Associated With Attention-Deficit/Hyperactivity Disorder Are  
358 Revealed by Leveraging Polygenic Overlap With Educational Attainment. *J. Am. Acad. Child*  
359 *Adolesc. Psychiatry* **57**, 86–95 (2018).
- 360 53. Bycroft, C. *et al.* The UK Biobank resource with deep phenotyping and genomic data. *Nature* **562**,  
361 203–209 (2018).
- 362 54. Bycroft, C. *et al.* Genome-wide genetic data on 500,000 UK Biobank participants. *bioRxiv* 166298  
363 (2017) doi:10.1101/166298.
- 364 55. Alfaro-Almagro, F. *et al.* Image processing and Quality Control for the first 10,000 brain imaging  
365 datasets from UK Biobank. *NeuroImage* **166**, 400–424 (2018).
- 366 56. Jenkinson, M., Beckmann, C. F., Behrens, T. E. J., Woolrich, M. W. & Smith, S. M. FSL. *20 YEARS*  
367 *FMRI* **62**, 782–790 (2012).

Roelfs et al. | Genetics of the brain functional connectome

- 368 57. Smith, S. M. *et al.* Advances in functional and structural MR image analysis and implementation as  
369 FSL. *NeuroImage* **23 Suppl 1**, S208-219 (2004).
- 370 58. Griffanti, L. *et al.* ICA-based artefact removal and accelerated fMRI acquisition for improved resting  
371 state network imaging. *NeuroImage* **95**, 232–247 (2014).
- 372 59. Salimi-Khorshidi, G. *et al.* Automatic denoising of functional MRI data: combining independent  
373 component analysis and hierarchical fusion of classifiers. *NeuroImage* **90**, 449–468 (2014).
- 374 60. Beckmann, C. F. & Smith, S. M. Probabilistic independent component analysis for functional  
375 magnetic resonance imaging. *IEEE Trans. Med. Imaging* **23**, 137–152 (2004).
- 376 61. Smith, S. M. *et al.* Functional connectomics from resting-state fMRI. *Spec. Issue Connect.* **17**, 666–  
377 682 (2013).
- 378 62. Kaufmann, T. *et al.* Task modulations and clinical manifestations in the brain functional connectome  
379 in 1615 fMRI datasets. *NeuroImage* **147**, 243–252 (2017).
- 380 63. Woolrich, M. W., Behrens, T. E. J., Beckmann, C. F., Jenkinson, M. & Smith, S. M. Multilevel linear  
381 modelling for fMRI group analysis using Bayesian inference. *NeuroImage* **21**, 1732–1747 (2004).
- 382 64. Otowa, T. *et al.* Meta-analysis of genome-wide association studies of anxiety disorders. *Mol.*  
383 *Psychiatry* **21**, 1391–1399 (2016).
- 384 65. Grove, J. *et al.* Identification of common genetic risk variants for autism spectrum disorder. *Nat.*  
385 *Genet.* **51**, 431–444 (2019).
- 386 66. Mullins, N. *et al.* Genome-wide association study of more than 40,000 bipolar disorder cases provides  
387 new insights into the underlying biology. *Nat. Genet.* **53**, 817–829 (2021).
- 388 67. Wray, N. R. *et al.* Genome-wide association analyses identify 44 risk variants and refine the genetic  
389 architecture of major depression. *Nat. Genet.* **50**, 668–681 (2018).
- 390 68. Duncan, L. E. *et al.* Largest GWAS of PTSD (N=20,070) yields genetic overlap with schizophrenia  
391 and sex differences in heritability. *Mol. Psychiatry* **23**, 666–673 (2018).
- 392 69. Pardiñas, A. F. *et al.* Common schizophrenia alleles are enriched in mutation-intolerant genes and in  
393 regions under strong background selection. *Nat. Genet.* **50**, 381–389 (2018).

Roelfs et al. | Genetics of the brain functional connectome

- 394 70. Chang, C. C. *et al.* Second-generation PLINK: rising to the challenge of larger and richer datasets.  
395 *Gigascience* **4**, 7 (2015).
- 396 71. Finucane, H. K. *et al.* Partitioning heritability by functional annotation using genome-wide  
397 association summary statistics. *Nat. Genet.* **47**, 1228–1235 (2015).
- 398 72. Bulik-Sullivan, B. K. *et al.* LD Score regression distinguishes confounding from polygenicity in  
399 genome-wide association studies. *Nat Genet* **47**, 291–5 (2015).
- 400 73. Bulik-Sullivan, B. *et al.* An atlas of genetic correlations across human diseases and traits. *Nat Genet*  
401 **47**, 1236–41 (2015).
- 402 74. Lee, J. J., McGue, M., Iacono, W. G. & Chow, C. C. The accuracy of LD Score regression as an  
403 estimator of confounding and genetic correlations in genome-wide association studies. *Genet.*  
404 *Epidemiol.* **42**, 783–795 (2018).
- 405 75. Loughnan, R. J. *et al.* Generalization of Cortical MOSTest Genome-Wide Associations Within and  
406 Across Samples. *bioRxiv* 2021.04.23.441215 (2021) doi:10.1101/2021.04.23.441215.

407  
408

409 **Online Methods**

410

411 *Sample and exclusion criteria*

412 We accessed resting state fMRI data from the UK Biobank<sup>53</sup>, a large-scale resource of imaging, genetics,  
413 and other biological and psychological data (access with permission no. 27412). All participants provided  
414 signed informed consent before inclusion in the study. The UK Biobank was approved by the National  
415 Health Service National Research Ethics Service (ref. 11/NW/0382). We selected data from individuals  
416 with White British ancestry, identified based on the genetic clustering performed by the UK Biobank  
417 team<sup>54</sup>. Data of all eligible participants were included for the main analysis in November 2020 and we did  
418 not exclude individuals based on a diagnosis. The resulting sample comprised data of 30,701 individuals  
419 with a mean age of 64.24 years (SD: 7.50, range: 45-82; 52.8% females). Additional data became  
420 available afterwards and was partly used for replication (see Replication section).

421

422 *Image acquisition and pre-processing*

423 Data had been acquired by the UK Biobank study team<sup>53</sup>. The fMRI images were collected on four  
424 identical 3T Siemens Magnetom Skyra scanners in the UK with a 32 channel head coil (Siemens  
425 Healthcare GmbH, Erlangen, Germany). Data was recorded using a gradient-echo echo planar imaging  
426 sequence with x8 multislice acceleration (TR: 0.735s, TE: 39ms, FOV: 88x88x64 matrix, FA: 52°) with a  
427 voxel size of 2.4x2.4x2.4mm. One fMRI sequence took approximately 6 minutes. The protocol further  
428 included T1 imaging, acquired using a MPRAGE sequence with in-plane acceleration (iPAT) of 2  
429 (resolution: 1mm<sup>3</sup>, FOV: 208x256x256 matrix).

430 Data had been preprocessed by the UK Biobank study team as described in Alfaro-Almagro *et al.*<sup>55</sup>.  
431 Briefly, their preprocessing used the FSL pipeline<sup>56,57</sup>, which included motion correction using MC-  
432 FLIRT (Jenkinson, Bannister, Brady, & Smith, 2002), grand-mean intensity normalization, high-pass  
433 filtering through Gaussian-weighted least-squares straight line fitting, EPI unwarping and GDC  
434 unwarping. Structured artifacts were removed using ICA and FIX<sup>58,59</sup>, where the FIX classifier was hand-  
435 trained on 40 UK Biobank datasets. According to Alfaro-Almagro *et al.* only 1% of variance in a scan is  
436 due to head motion following motion correction and FIX<sup>55</sup>. The final step was a group ICA using  
437 MELODIC<sup>60</sup> which decomposed the data using independent component analysis into 25 components.

438 We retrieved individual level time series data for each subject and component (output from dual  
439 regression at model order 25). We computed functional brain networks using the FSLNets toolbox<sup>61</sup>. First,  
440 we regressed the time series of four noise components from the time series of the remaining 21  
441 components and subsequently removed those four components. Suppl. Fig. 9 depicts maps for each of the  
442 21 components. We estimated functional connectivity (FC) as the regularized partial correlations of the  
443 component time series, implementing an approach developed by Ledoit & Wolf (2012) which performs an  
444 automated adjustment of the shrinkage parameter lambda, as implemented in our earlier work<sup>62</sup>. As the  
445 last step, we regressed age, age<sup>2</sup>, sex, scanner, motion, signal-to-noise ratio (SNR), and the first 20 genetic  
446 principal components from the individual connection strengths, residualizing each edge (210 in total) of  
447 the partial correlation matrix. In addition to functional brain connectivity, we also performed an analysis  
448 of the variance in signal amplitude of the 21 components<sup>56</sup>, and performed the same residualisation in this  
449 node-level analysis as described above for the edge level.

450 To test if our results were largely dependent on the pipelines used to define brain networks, we  
451 complemented our main data-driven ICA approach with a region-of-interest (ROI) approach using the  
452 Schaefer parcellation with 1000 parcels. For this pipeline we accessed FEAT<sup>63</sup> processed folders from the  
453 UK Biobank and registered all images to standard MNI space. For each Schaefer-defined ROI there exists  
454 a mapping to the 17 large-scale brain networks defined by Yeo et al (2011). To achieve comparability to  
455 our main ICA-based analysis, which comprises 21 network nodes, we averaged the time series of all  
456 Schaefer-defined ROIs corresponding to each Yeo-defined network, yielding ROI-based networks with 17

## Roelfs et al. | Genetics of the brain functional connectome

457 nodes. Following the standard procedure for ROI-based brain networks, we defined these as the Pearson  
458 correlation of the 17 nodal time series. Furthermore, we derived node variance of these 17 nodes. The  
459 resulting functional brain connectivity as well as node variances went into the same genetic analyses as  
460 performed in the main ICA-based analysis workflow.

461  
462 *Genetic data and QC*  
463 We accessed UKB v3 imputed data<sup>53</sup>. The data acquisition and preprocessing pipeline is described in  
464 Bycroft *et al.*<sup>53</sup>. We applied standard quality control procedures to this data and removed SNPs with a  
465 minor allele frequency below 0.001, SNPs missing in more than 5% of individuals, SNPs with an  
466 imputation quality below 0.5, and SNPs failing the Hardy-Weinberg equilibrium test at  $P < 1e-9$ .

467  
468 *Univariate and Multivariate Genome-Wide Analysis*  
469 We performed multivariate and univariate GWAS using the Multivariate Omnibus Statistical Test  
470 (MOSTest)<sup>29</sup>. MOSTest takes as input all univariate test statistics (z-scores) for each SNP, as obtained  
471 through standard association testing with each pre-residualized phenotype, and compares this to test  
472 statistics obtained following a single random permutation of the genotype vector. A multivariate test  
473 statistic is then calculated from this comparison as the Mahalanobis norm, with the probability of the  
474 observed test-statistic being derived from a Chi-square distribution. Further details of the method are  
475 described in Van der Meer *et al.*<sup>29</sup>. MOSTest returns a multivariate test statistic, where in contrast to  
476 classical univariate GWAS that link a given SNP with a single phenotype, for each SNP the multivariate  
477 association across all included phenotypes is provided. This allowed us to retrieve one multivariate  
478 summary statistic for functional brain connectivity (edge level), and one for node variance (node level). In  
479 addition, we retrieved classical univariate summary statistics for follow-up analyses.

480  
481 *Summary statistics for psychiatric disorders*  
482 We accessed publicly available summary statistics for Attention-Deficit Hyperactivity Disorder  
483 (ADHD)<sup>51</sup>, anxiety disorder (ANX)<sup>64</sup>, autism spectrum disorder (ASD)<sup>65</sup>, bipolar disorder (BIP)<sup>66</sup>, major  
484 depression (MD)<sup>67</sup>, Post-Traumatic Stress Disorder (PTSD)<sup>68</sup>, and schizophrenia (SCZ)<sup>69</sup>. For details, see  
485 Suppl. Table 1. We used vitamin D<sup>34</sup> as a negative control phenotype because it is well powered (N =  
486 79,366), has heritability comparable to psychiatric disorders ( $h^2_{\text{twin}} \sim 0.6$ ) and is not genetically correlated  
487 with the included psychiatric disorders (all  $P > .05$ ). We performed a GWAS using plink 2.0<sup>70</sup> on 79,366  
488 participants in the UK Biobank not included in the main analysis.

489  
490 *Pleiotropy-informed conjunctive false discovery rate*

## Roelfs et al. | Genetics of the brain functional connectome

491 Due to the complex and polygenic architecture of our brain phenotypes, we utilized pleiotropy-informed  
492 conjunctural false discovery rate (conjFDR) as implemented in the pleioFDR toolbox<sup>35</sup>. The conjFDR  
493 identifies shared genomic loci between two traits regardless of effect directionality and effect size, making  
494 it ideally suited to compare a multivariate summary statistic from MOSTest (here: FC and variance)  
495 against the summary statistics of a given disorder (here: SCZ, BD, MD, ASD, ADHD, ANX, PTSD).

496  
497 *Linkage Disequilibrium Score Regression*  
498 For the univariate summary statistics, we estimated partitioned heritability<sup>71</sup> and genetic correlation with  
499 LD-score regression using the LDSC tool<sup>72</sup>. We also estimated genetic correlation between each edge and  
500 variance across time in each node with the seven psychiatric disorders using cross-trait LDSC<sup>72-74</sup>. Of  
501 note, genetic correlations require effect directions and are thus not applicable to the multivariate summary  
502 statistics derived from MOSTest. We therefore used genetic correlations in connection with univariate  
503 statistics as a complement to the multivariate pipeline.

504  
505 *Gene mapping and annotation*  
506 We used the Functional Mapping and Annotation (FUMA version v1.3.6a) tool to map loci derived  
507 through conjunctural FDR analyses to genes and tested for significant enrichment of biological  
508 processes<sup>36</sup>. We then fed the genes identified through FUMA into the *SynGO* (v1.1) toolbox to map  
509 synaptic genes<sup>37</sup>, and the *reactome* (v78) toolbox to map the genes to a range of biological processes<sup>40</sup>.

510  
511 *Replication*  
512 To validate the discovered loci of the functional brain measures, we performed a replication analysis of  
513 our two main MOSTest analyses on a dataset containing all subjects with available data (including those  
514 with non-White British ancestry) as well as a new batch of data (including White British) that arrived after  
515 we performed the main analyses. This resulted in a dataset containing 9175 individuals, which we  
516 processed in the same way as the data from the discovery sample. Multivariate discoveries require a  
517 special replication procedure to ensure that a locus in question is not only showing an association in an  
518 independent sample, but also that the multivariate pattern of that association is consistent between the  
519 discovery and the replication samples. Such procedure has been established in Loughnan et al.<sup>75</sup> For a  
520 given SNP in the discovery set, the procedure provides a composite score (one value for each individual in  
521 the validation set) obtained as a weighted sum of individuals' phenotypes, with weights derived from  
522 mass-univariate z-statistics from the discovery set. If a SNP association represents a real signal in the  
523 discovery set, we expect its composite score to be associated with the genotype in the replication sample  
524 at a nominal one-sided  $P < 0.05$ , and to have a consistent effect direction. Mathematical formulation of the  
525 approach is provided in Loughnan et al.<sup>75</sup>

## Roelfs et al. | Genetics of the brain functional connectome

526

### 527 *Acknowledgements*

528 The authors were funded by the Research Council of Norway (#276082 LifespanHealth, #323961  
529 BRAINGAP, #223273 NORMENT, #283798 ERA-NET Neuron SYNSCHIZ, #249795, #298646,  
530 #300767), the South-East Norway Regional Health Authority (2019101, 2019107, and 2020086), and the  
531 European Research Council under the European Union's Horizon2020 Research and Innovation program  
532 (ERC Starting Grant #802998), as well as the Horizon2020 Research and Innovation Action Grant  
533 CoMorMent (#847776). This research has been conducted using the UK Biobank Resource (access code  
534 27412, <https://www.ukbiobank.ac.uk/>). This work was performed on the TSD (Tjenester for Sensitive  
535 Data) facilities, owned by the University of Oslo, operated and developed by the TSD service group at the  
536 University of Oslo, IT-Department (USIT). Computations were also performed on resources provided by  
537 UNINETT Sigma2 - the National Infrastructure for High Performance Computing and Data Storage in  
538 Norway.

539

### 540 *Conflicts of interest*

541 D.R., D.vd.M., D.A., O.F., A.A.S., R.L., C.C.F., L.T.W. and T.K. declare no conflicts of interest. O.A.A.  
542 is a consultant to HealthLytix and received speakers honorarium from Lundbeck. A.M.D. is a Founder of  
543 and holds equity in CorTechs Labs, Inc, and serves on its Scientific Advisory Board. The terms of this  
544 arrangement have been reviewed and approved by UCSD in accordance with its conflict of interest  
545 policies.

546

### 547 *Author contributions*

548 D.R. and T.K. conceived the study; D.R. analyzed the data with contributions from T.K.; All authors  
549 contributed with conceptual input on methods and/or interpretation of results; D.R. and T.K. wrote the  
550 first draft of the paper and all authors contributed to the final manuscript.

551

### 552 *Data availability*

553 Data used in this study are part of the publicly available UK Biobank initiative  
554 (<https://www.ukbiobank.ac.uk/>). Summary statistics for the disorders are publicly available through their  
555 respective consortia (Suppl. Table 1). The summary statistics for the multivariate analyses will be shared  
556 on GitHub (<https://www.github.com/norment/open-science>) upon acceptance.

557

### 558 *Code availability*

559 Code will be made publicly available via GitHub (<https://www.github.com/norment/open-science>) upon  
560 acceptance of the manuscript.